

Multi-Scale Diffusion: Enhancing Spatial Layout in High-Resolution Panoramic Image Generation

Xiaoyu Zhang, Teng Zhou, Xinlong Zhang, Jia Wei, Yongchuan Tang *

Zhejiang University, HangZhou, China
 {xiaoyzhang, 12421050, xinlzhang, weijia.77, yctang}@zju.edu.cn

Abstract

Diffusion models have recently gained recognition for generating diverse and high-quality content, especially in the domain of image synthesis. These models excel not only in creating fixed-size images but also in producing panoramic images. However, existing methods often struggle with spatial layout consistency when producing high-resolution panoramas, due to the lack of guidance of the global image layout. In this paper, we introduce the Multi-Scale Diffusion (MSD) framework, a plug-and-play module that extends the existing panoramic image generation framework to multiple resolution levels. By utilizing gradient descent techniques, our method effectively incorporates structural information from low-resolution images into high-resolution outputs. A comprehensive evaluation of the proposed method was conducted, comparing it with the prior works in qualitative and quantitative dimensions. The evaluation results demonstrate that our method significantly outperforms others in generating coherent high-resolution panoramas.

1 Introduction

Diffusion models have recently demonstrated powerful generative capabilities in image synthesis (Ho, Jain, and Abbeel 2020; Dhariwal and Nichol 2021; Song, Meng, and Ermon 2020). These models construct dual Markov chains to learn data distributions by simulating diffusion and denoising processes. They generate high-quality images that surpass those generated by other generative models. (Kobyzev, Prince, and Brubaker 2020; Karras, Laine, and Aila 2019; Van Den Oord, Vinyals et al. 2017). Notable examples such as Stable Diffusion (Ramesh et al. 2022; Podell et al. 2023), trained on extensive, diverse datasets, have substantially advanced the field. These models excel in producing detailed, contextually accurate images, thereby establishing themselves as pivotal components in generative AI with wide-ranging applications.

Panoramic image generation (Bar-Tal et al. 2023; Feng et al. 2023; Zhou et al. 2024) produces images with variable aspect ratios. This technology provides an expansive field of view, enhancing visual completeness and immersion. Despite receiving considerable research attention, this field faces several challenges, particularly the limited availability

of training data. The scarcity of data impedes the ability of diffusion models to generate panoramic images directly.

To address this challenge, existing methods stitch together images generated by multiple diffusion models. These methods fall into two categories: image extrapolation (Avrahami, Lischinski, and Fried 2022; Avrahami, Fried, and Lischinski 2023) and joint diffusion (Zhang et al. 2023; Tang et al. 2023; Jiménez 2023). Joint diffusion has become the leading method for seamless panoramic image generation. This approach integrates models with shared parameters or constraints, blending noisy images across overlapping regions by averaging the intermediate outputs at each denoising step. A notable example is the MultiDiffusion (MD) (Bar-Tal et al. 2023), which represents a significant advancement in this field and is capable of producing realistic, seamless panoramas. However, the MD framework exhibits limitations in generating high-resolution panoramas. The absence of global layout guidance leads to a disorganized spatial arrangement, compromising the overall quality of the final images (Fig. 1).

To address the challenges of generating high-resolution panoramic images, we propose Multi-Scale Diffusion (MSD) module. The core concept involves integrating the overall structure and composition from lower-resolution images with details extracted from higher resolutions. Within a single-step denoising process, the procedure is divided into multiple stages, employing a phased strategy that progressively enhances the panoramic image’s clarity. At each resolution level, the module builds upon the MultiDiffusion technique for joint denoising. By utilizing low-resolution images as structural guides through gradient descent optimization, MSD effectively reduces inconsistencies across different resolution layers. As illustrated in Fig. 1, our method successfully generates panoramic images with large-scale coherence and fine-grained accuracy.

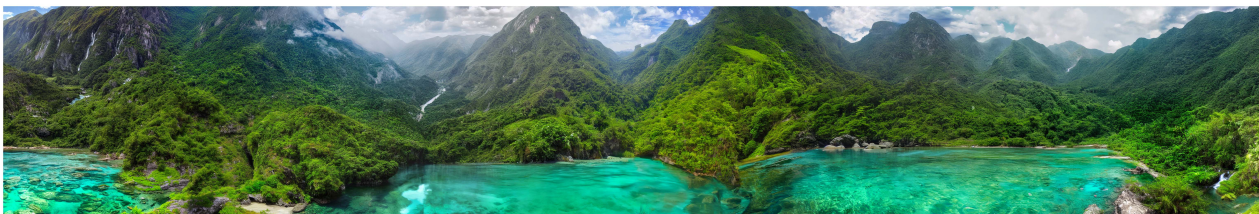
We evaluate the MSD model’s performance against established baselines using both quantitative and qualitative measures. The model was quantitatively assessed in terms of diversity and fidelity using FID (Heusel et al. 2017) and KID (Bińkowski et al. 2018), as well as semantic compatibility using CLIP (Radford et al. 2021) and CLIP-Aesthetic metrics (Schuhmann et al. 2022). The MSD model consistently outperformed baselines across all metrics, particularly excelling in KID and FID, which reflect diversity and re-

"Clear waters and green mountains"

MD

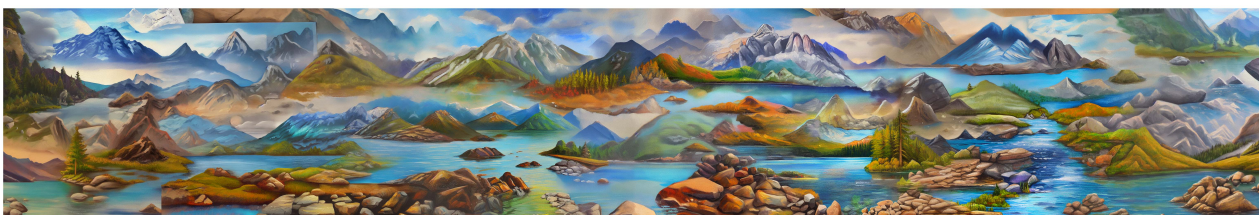


Ours



"Mountains, lakes and stones in oil paintint style"

MD



Ours

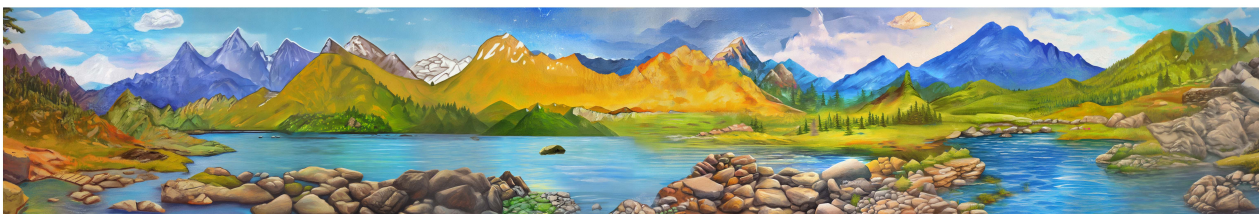


Figure 1: Comparison of high-resolution panoramic images generated by MultiDiffusion and our Multi-Scale Diffusion under different prompts. MultiDiffusion excels in seamless image stitching but struggles with spatial coherence, leading to structural inconsistencies. In contrast, our model improves on this by integrating coarse structures and fine details from different resolution levels, producing panoramas that are both structurally coherent and visually detailed.

alism. Qualitatively, it generated high-resolution panoramic images that are more visually and semantically coherent across diverse textual prompts. These results establish the MSD model’s superiority in high-resolution panoramic image synthesis.

The main contributions of our work are as follows:

- We identify the integration of global layout information as essential for producing high-quality, high-resolution panoramic images.
- Building on our theoretical findings, we propose the Multi-Scale Diffusion (MSD) framework. Our method incorporates spatial guidance via gradient descent, producing panoramas that are both structurally coherent and rich in detail.
- Comprehensive experiments validate the effectiveness of our approach, which surpasses baselines in both quantitative metrics and qualitative evaluations, solidifying it as a superior solution for panoramic image generation.

2 Related Work

2.1 Diffusion Models

Diffusion models (Sohl-Dickstein et al. 2015; Dhariwal and Nichol 2021; Song et al. 2020; Nichol and Dhariwal 2021) represent a class of generative models that create data through a two-step process: forward diffusion and reverse denoising. This process uses Markov chains to gradually alter and reconstruct data distributions, enabling the creation of data from noise in a step-by-step manner.

The field has seen significant advancements since the emergence of DDPM (Ho, Jain, and Abbeel 2020). These models have become particularly successful in image generation (Saharia et al. 2022; Dhariwal and Nichol 2021), outperforming previous approaches like GANs (Karras et al. 2020; Karras, Laine, and Aila 2019), VAEs (Kingma and Welling 2013; Van Den Oord, Vinyals et al. 2017) and Flows (Kobyzev, Prince, and Brubaker 2020). DDIM (Song, Meng, and Ermon 2020) further improved the process by

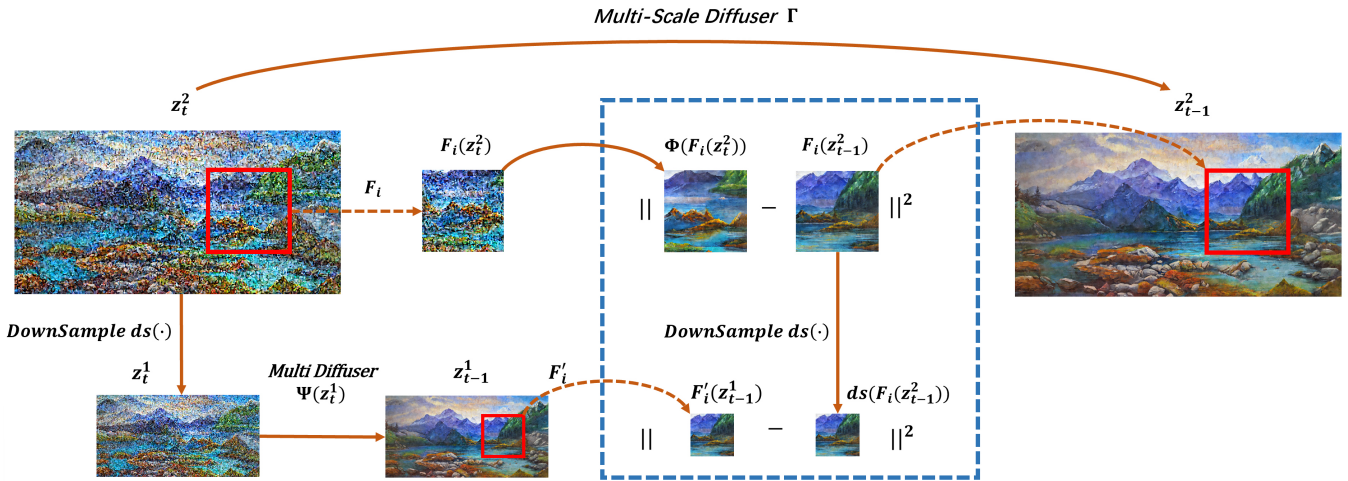


Figure 2: Our MSD module framework. The single-step denoising process is clarity into multiple stages, progressively denoising the panoramic image from low to high resolution. Building on the pre-trained model, denoted as Φ , a new generation method, called Γ , is introduced. This method uses the results from the low-resolution denoising as constraints to guide the high-resolution denoising. The optimization objectives are twofold: (i) ensuring the final denoised image $F_i(\Gamma(z_t^2))$ closely matches the denoised results of each cropped window $\Phi(F_i(z_t^2))$; (ii) maintaining consistency between denoised images across different resolution layers (z_t^2, z_{t-1}^1). For the lowest-resolution image, our method simplifies to the standard MultiDiffusion approach, denoted by Ψ .

introducing non-Markovian transitions that predict denoised data, significantly accelerating the denoising process. Another major development came with LDM (Rombach et al. 2022), which moved the diffusion process into latent space using a pre-trained autoencoder. This innovation led to high-performance models like Stable Diffusion (Rombach et al. 2022; Podell et al. 2023) and DALLE2 (Ramesh et al. 2022).

The success of diffusion models has expanded their application beyond images. They are now being used to generate various types of content, including audio (Yang et al. 2023; Huang et al. 2023; Liu et al. 2023; Ghosal et al. 2023), video (Ho et al. 2022; Blattmann et al. 2023; Liu et al. 2024), and 3D objects (Xu et al. 2023; Lin et al. 2023; Poole et al. 2022), demonstrating their versatility in creating different forms of multimodal data.

2.2 Panoramic Image Generation

The use of diffusion models for panoramic image generation has garnered significant research attention. Due to challenges in data acquisition and computational efficiency, directly generating panoramas presents numerous difficulties. Existing methods can be mainly divided into two categories: image extrapolation methods (Avrahami, Lischinski, and Fried 2022; Avrahami, Fried, and Lischinski 2023), which extrapolate image edges, and approaches that integrate multiple diffusion paths to fuse overlapped denoising paths without additional training or fine-tuning (Jiménez 2023; Zhang et al. 2023; Tang et al. 2023).

The MultiDiffusion (Bar-Tal et al. 2023) exemplifies the second category of diffusion models, proving to be feasible and effective. It has laid a foundation for numerous subsequent studies. SCALECRAFTER (He et al. 2023) adapts

diffusion models for higher resolutions by dilating convolution kernels at specific layers. Demofusion (Du et al. 2024) employs an “upsample-diffuse-denoise” loop to progressively convert low-resolution images to high-resolution ones. However, these methods focus on generating high-resolution images rather than panoramic ones. SyncDiffusion (Lee et al. 2023) ensures consistent quality across panoramic images by calculating perceptual loss across multiple windows. TwinDiffusion (Zhou and Tang 2024) achieves smoother transitions and fewer seams by tightly aligning adjacent parts of the panoramic image space. Nevertheless, these methods are limited to generating scene images repetitively in either the length or width direction. When extending in both directions simultaneously, conflicting scene layouts in different windows result in a chaotic overall image layout.

To address this issue, we build upon existing methods by incorporating guidance from low-resolution images to capture structural details. This approach enables the generation of panoramas that are both rich in detail and structurally sound.

3 Method

3.1 Preliminary

Latent Diffusion Model. We introduce a pre-trained diffusion model operating in a latent space $\mathbb{R}^{c \times h \times w}$. The model generates image z_0 through iterative denoising, starting with initial Gaussian noise z_T . This process follows a predefined noise schedule, updating the current image z_t at each timestep t with the following formula:

$$x_{t-1} = \sqrt{\alpha_{t-1}} \left(\frac{x_t - \sqrt{1 - \alpha_t} \epsilon_\theta(x_t, t)}{\sqrt{\alpha_t}} \right) + \sqrt{1 - \alpha_{t-1}} \epsilon_\theta(x_t, t), \quad (1)$$

where α_t is parameterized by the noise schedule, $\epsilon_\theta(x_t, t)$ is the noise predicted by the denoising model at timestep t , parameterized by θ . For brevity, we denote the denoising steps as Φ in the rest of the paper:

$$z_{t-1} = \Phi(z_t), \quad (2)$$

MultiDiffusion. The MultiDiffusion (Bar-Tal et al. 2023) framework extends LDMs (Rombach et al. 2022) by employing a multi-window joint diffusion technique. In this approach, the denoising process of the model Ψ is conducted a latent space $\mathbb{R}^{c \times H \times W}$ with $H > h$ and $W > w$. Initially, the panoramic image $z_t \in \mathbb{R}^{c \times H \times W}$ is cropped into a series of window images:

$$x_t^i = F_i(z_t), \quad (3)$$

where $F_i(\cdot)$ refers to cropping the i -th image patch from image z_t .

Subsequently, each window undergoes independent denoising according to Eq. 2. The objective of MultiDiffuser is to ensure that $\Psi(z_t)$ closely aligns with $\Phi(x_t^i)$, $i \in [n]$. Therefore, the optimization problem is defined as follows:

$$z_{t-1} = \operatorname{argmin}_{\hat{z}_{t-1}} \mathcal{L}_{MD}(\hat{z}_{t-1} | z_t), \quad (4)$$

$$\mathcal{L}_{MD} = \sum_{i=1}^N W_i \otimes \|F_i(\hat{z}_{t-1}) - \Phi(F_i(z_t))\|^2, \quad (5)$$

where \hat{z}_{t-1} represents the variable to be determined in relation to z_t and W_i denote the weight matrix of the i -th window.

The framework then utilizes a global least squares method to integrate the denoising outcomes from each window. Thus, the final image is computed as a weighted average value:

$$z_{t-1} = \frac{\sum_i W_i \otimes F_i^{-1}(\Phi(x_t^i))}{\sum_i W_i}, \quad (6)$$

where $F_i^{-1}(\cdot)$ is the inverse function of $F_i(\cdot)$.

3.2 Multi-Scale Diffusion

MultiDiffusion effectively generates coherent panoramic images when expanding in a single dimension, such as vertically. However, it struggles with simultaneous horizontal and vertical expansions, often resulting in unintended image convergences and visual inconsistencies. These issues arise because the model generates different panorama segments independently, leading to misaligned features and repetitive patterns, as shown in Fig. 1. The lack of contextual awareness between segments disrupts spatial logic, reducing the overall realism and coherence of the image. This limitation

underscores the need for a more integrated approach to complex panoramic generation across both dimensions.

To address this issue, we propose a Multi-Scale Diffusion model, enabling the generation of coherent and highly detailed panoramic images, as shown in Fig. 2. This module can be integrated into existing joint diffusion frameworks. By extending the MultiDiffusion approach across multiple resolution layers, it balances the creation of semantically coherent structures at lower resolutions with the capture of intricate details at higher resolutions, improving overall image quality. The optimization task is defined as:

$$\begin{aligned} z_{t-1}^s &= \operatorname{argmin}_{\hat{z}_{t-1}^s} \mathcal{L}_{MSD}(\hat{z}_{t-1}^s | z_t^s, z_{t-1}^{s-1}) \\ &= \operatorname{argmin}_{\hat{z}_{t-1}^s} \mathcal{L}_{MD}(\hat{z}_{t-1}^s | z_t^s) + \omega \mathcal{L}_{MS}(\hat{z}_{t-1}^s | z_{t-1}^{s-1}), \end{aligned} \quad (7)$$

where z_t^s denotes the noise image at the s -th resolution, ω is the weight. The equation comprises two components: \mathcal{L}_{MD} represents the optimization objective of MultiDiffusion (Eq. 5), while \mathcal{L}_{MS} ensures minimal deviation between denoised images across different resolution layers. The formula is as follows:

$$\mathcal{L}_{MS} = \sum_{i=1}^N W_i \otimes \|ds(F_i(\hat{z}_{t-1}^s)) - F_i'(z_{t-1}^{s-1})\|^2, \quad (8)$$

where $ds(\cdot)$ refer to the downsampling function (e.g., Bilinear Interpolation), and $F_i'(\cdot)$ is the crop function associated with $F_i(\cdot)$ that samples the corresponding region on the low-resolution panoramic image z_{t-1}^{s-1} . In contrast to MultiDiffusion, which derives an analytical solution for z_{t-1}^s by averaging features in overlapping regions, we employ back-propagation of gradients to obtain an approximate solution for z_{t-1}^s .

During the single-step denoising of the noisy image z_t^S , we sequentially downsample the image, creating a series of progressively lower-resolution images, culminating in the lowest-resolution image z_t^0 . We divide the denoising process into S stages, progressively applying the Multi-Scale Diffusion to the noisy image z_t^s from low to high resolution, except for the first phase which applies MultiDiffusion for denoising.

At each resolution level s (where $s > 1$), the MSD module crops the noisy image z_t^s using the cropping function $F_i(\cdot)$, resulting in a window image $x_{t,i}^s$. This image is then denoised, producing the denoised window image $\Phi(x_{t,i}^s)$. Concurrently, the module applies the cropping function $F_i'(\cdot)$ to the low-resolution panoramic image z_{t-1}^{s-1} , generating another window image $x_{t-1,i}^{s-1}$, which corresponds to $x_{t,i}^s$.

Theoretically, the denoised and downsampled window image $\Phi(x_{t,i}^s)$ should closely resemble the window image $x_{t-1,i}^{s-1}$, which is created by downsampling first and then denoising. The module calculates the mean squared error between the two window images, which serves as the loss function. It then computes the gradient and applies backpropaga-

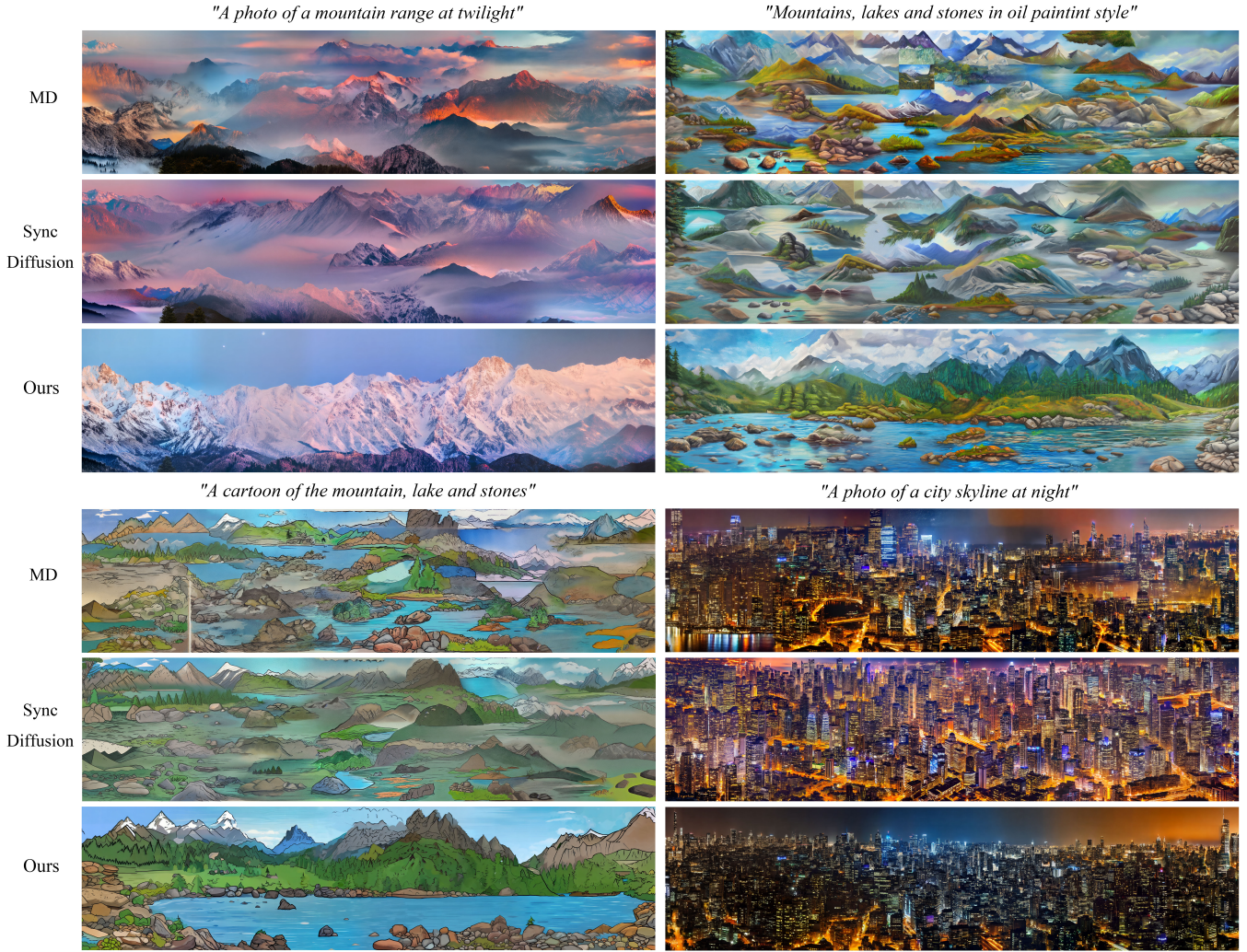


Figure 3: Qualitative comparisons among MultiDiffusion, SyncDiffusion, Multi-Scale Diffusion. Our approach significantly improves spatial layout issues in high-resolution panoramic generation, producing semantically coherent and visually consistent results.

tion to update the original window image $x_{t,i}^s$. The specific formula is provided below:

$$\hat{x}_{t,i}^s = x_{t,i}^s - \omega \nabla_{x_{t,i}^s} \left\| ds \left(\Phi \left(x_{t,i}^s \right) \right) - x_{t-1,i}^{s-1} \right\|^2, \quad (9)$$

where ω is the weight of the gradient descent. MultiDiffusion is applied to denoise and merge these images at the end, according to Eq.6. Refer to Alg. 1 in the Appendix for the detailed pseudocode.

4 Experiment

4.1 Experimental Setting

Baselines We compare our MSD model with the following two baseline models: (1) MultiDiffusion (Bar-Tal et al. 2023), a special case of our method when the gradient weight $\omega = 0$; (2) SyncDiffusion (Lee et al. 2023), which

enhances global consistency based on MultiDiffusion by incorporating perceptual loss. For a fair comparison, identical hyperparameters were used across all models, and the experiments were conducted using an A100 GPU.

Experimental Setup We employ the Stable Diffusion (SD) v2.0 model as the reference model. Operating within a latent space of $\mathbb{R}^{4 \times 64 \times 64}$, this model generates images of $\mathbb{R}^{3 \times 512 \times 512}$. We aligned the crop window size with the model’s default resolution and generated panoramic images of resolution 1024×4096 (128×512 in the latent space). The panoramic images’ height is doubled, and the width is octupled compared to the original dimensions. The stride of the window is 32, resulting in 52 segmented windows: 45 high-resolution and 7 low-resolution windows.

Section 4.2 presents results using specific parameters: gradient weight of $\omega = 10$, scaled cosine decay factor of $(1 + \cos(\frac{T-t}{T} \times \pi)) / 2$, and the termination of gradient de-

scent at $\tau = 7/10T$. Section 4.3 provides a detailed analysis of how these parameters affect image generation.

Datasets To ensure the reliability of our results, we utilized eight distinct textual prompts covering a variety of themes and artistic styles, generating 500 panoramic images for each prompt. To meet the dimensional requirements of the evaluation metrics, we sampled several 1024×1024 pixel crops from the panoramas and used these as our test datasets, following a common approach in this field (Bar-Tal et al. 2023; Lee et al. 2023; Zhou and Tang 2024). Additionally, a reference dataset comprising 2,000 images per prompt was generated using Stable Diffusion.

4.2 Comparison

We conducted a comprehensive evaluation of our MSD model compared to baseline models, encompassing both qualitative and quantitative aspects.

Qualitative Comparison Fig. 3 compares images generated by the proposed method and two baseline models. While the MultiDiffusion model stitches scenes well, it leads to disorganized layouts and unnatural features in high-resolution panoramic images. The SyncDiffusion model improves stylistic consistency but suffers from spatial structure issues like floating mountains and unsupported lakes. These observations highlight that optimizing window connections and maintaining style consistency alone is insufficient for high-quality panoramic image generation.

In contrast, our MSD method generates high-resolution panoramic images that are more visually and semantically coherent across all textual prompts. The improvement in image quality correlates positively with the spatial logic of the textual prompts, demonstrating our method’s effectiveness in leveraging textual guidance to inform the spatial structure of generated images.

Quantitative Comparison We employ a variety of metrics to evaluate the generated panoramas. These metrics assess the fidelity and diversity of the panoramas, as well as their compatibility with the input prompts.

- **Fidelity & Diversity:** **FID** and **KID** were used to evaluate the fidelity and diversity of panoramic images. Both metrics compare the distribution of generated images to that of real images, with FID using feature vector distances and KID employing a kernel-based approach.
- **Compatibility:** **CLIP** was used to evaluate the alignment between image and text by calculating cosine similarity, while **CLIP-aesthetic** was used to quantify the aesthetic quality of the images using a linear estimator.

The quantitative comparison illustrated in Fig. 4 indicates that our MSD approach outperforms the baselines across four critical evaluation metrics. The color bars represent average scores, while the black lines denote standard deviation. Our method significantly improves image quality in panorama generation, as evidenced by enhanced FID and KID scores, which suggest that the images generated by our model more closely resemble those produced by the reference model. The CLIP-Aesthetic scores further corroborate

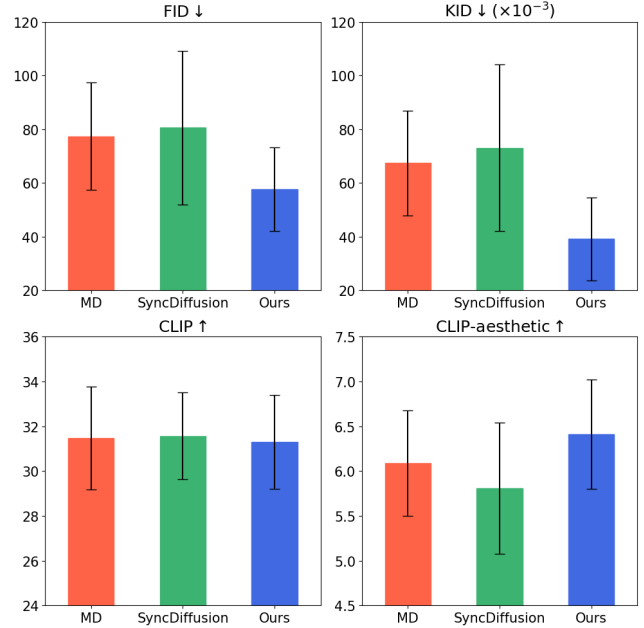


Figure 4: Quantitative results comparing four key metrics across two dimensions. Our method achieves the best overall performance, particularly in image quality, establishing it as the optimal choice for high-resolution panoramic image generation.

these improvements, with our method achieving the highest ratings. Additionally, our approach maintains compatibility with input prompts, performing comparably with other methods in the CLIP metric. In summary, our method effectively balances aesthetic quality with prompt relevance, making it a reliable solution for generating high-quality panoramas.

4.3 Ablation Study

Our MSD module includes several key factors that significantly influence its performance, such as the gradient weight and the timestep τ , which determines the termination of gradient backpropagation.

Gradient Weight The gradient weight ω in Eq. 9 is crucial for optimizing the spatial layout of high-resolution panoramic images. Adjusting ω controls the influence of spatial information from low-resolution images on their high-resolution counterparts, directly impacting final image quality. Our experiments revealed significant improvements in FID scores. Given FID’s importance in image quality assessment, we streamlined the evaluation process while maintaining focus on this critical metric.

Fig. 5 illustrates the impact of varying the gradient weight ω from 0 to 24. For $\omega \leq 2$, the FID metric decreases rapidly, indicating improved image layout. When $\omega \geq 20$, the FID metric increases, suggesting that excessive optimization leads to a collapse in image generation and a decline in quality. The optimal value for ω is 10, where the generated high-resolution images exhibit the best performance

in terms of both layout and detail.

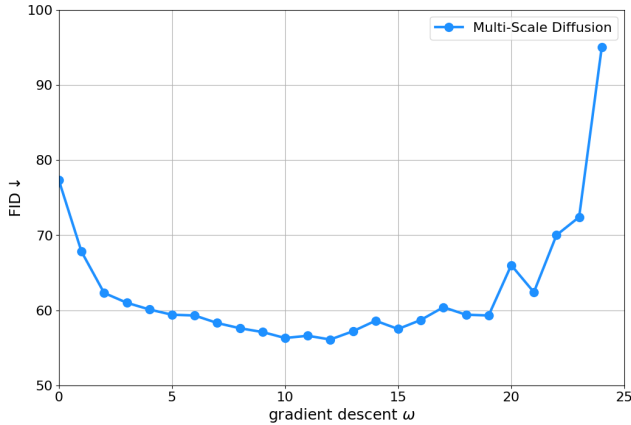


Figure 5: Impact of gradient weight ω on fidelity and diversity in high-resolution image generation. Optimal balance is achieved when $\omega = 10$. Lower ω values result in insufficient spatial layout optimization, while higher values may lead to image structure collapse.

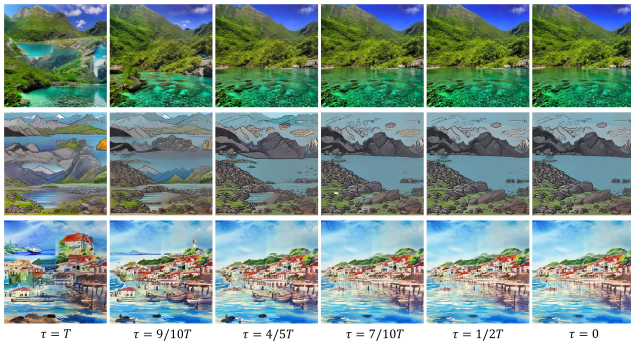


Figure 6: Impact of gradient descent cutoff time τ on image layout and generation efficiency. Decreasing τ stabilizes image layout, with convergence rates varying across prompts. At $\tau = 7/10T$, image quality is maintained while effectively controlling generation time, optimizing the balance between quality and efficiency.

Optimization Timestep Global optimization enhances image quality but is computationally intensive due to gradient backpropagation complexity. In the Stable Diffusion model, early denoising stages shape image layout and structure, and the impact of optimization diminishes later on in our model. To improve efficiency, we propose focusing optimization on the early stages of denoising, accelerating high-resolution panorama generation without sacrificing quality, and reducing computational demands for practical use. Consequently, we limit optimization to the initial denoising stages, applying gradient optimization during the time interval $t : T \rightarrow \tau$ and halting it during $t : \tau \rightarrow 0$, where T represents the total timestep of the diffusion scheduler.

Fig 6 illustrates the impact of the parameter τ on the spatial layout of high-resolution images. The observations indicate that image layout improves significantly with increasing τ during the early denoising stages and then stabilizes in the later stages. Although optimization speed varies depending on the prompt, layout optimization generally achieves the best results when τ is set to $7/10T$, after which further improvements become negligible.

5 Conclusion

The Multi-Scale Diffusion module is a versatile, integrable component that enhances image generation models’ capacity to produce high-resolution panoramic images. Operating across multiple resolution levels, it leverages information from low-resolution images to refine high-resolution outputs through gradient descent. This process yields panoramas that are both structurally coherent and rich in detail. Empirical evaluations demonstrate that MSD outperforms baseline methods both quantitatively and qualitatively. Beyond static images, the module shows potential for video generation, which we aim to explore in future research.

Limitations and Social Impact Our MSD module is effective across various scenarios but faces limitations. Its performance depends on the quality of images produced by the reference model and precise input prompts. The module also demands significant computational resources due to iterative gradient descent. Additionally, there are risks of misuse, such as generating unethical or misleading content. Future research must focus on enhancing model efficiency while promoting responsible use, including implementing safeguards against unethical applications and ensuring compliance with legal and societal norms.

References

- Avrahami, O.; Fried, O.; and Lischinski, D. 2023. Blended latent diffusion. *ACM transactions on graphics (TOG)*, 42(4): 1–11.
- Avrahami, O.; Lischinski, D.; and Fried, O. 2022. Blended diffusion for text-driven editing of natural images. In *Proceedings of the IEEE/CVF conference on computer vision and pattern recognition*, 18208–18218.
- Bar-Tal, O.; Yariv, L.; Lipman, Y.; and Dekel, T. 2023. MultiDiffusion: Fusing Diffusion Paths for Controlled Image Generation. In *International Conference on Machine Learning*.
- Bińkowski, M.; Sutherland, D. J.; Arbel, M.; and Gretton, A. 2018. Demystifying mmd gans. *arXiv preprint arXiv:1801.01401*.
- Blattmann, A.; Rombach, R.; Ling, H.; Dockhorn, T.; Kim, S. W.; Fidler, S.; and Kreis, K. 2023. Align your latents: High-resolution video synthesis with latent diffusion models. In *Proceedings of the IEEE/CVF Conference on Computer Vision and Pattern Recognition*, 22563–22575.
- Dhariwal, P.; and Nichol, A. 2021. Diffusion models beat gans on image synthesis. *Advances in neural information processing systems*, 34: 8780–8794.

- Du, R.; Chang, D.; Hospedales, T.; Song, Y.-Z.; and Ma, Z. 2024. Demofusion: Democratising high-resolution image generation with no \$\$\$\$. In *Proceedings of the IEEE/CVF Conference on Computer Vision and Pattern Recognition*, 6159–6168.
- Feng, M.; Liu, J.; Cui, M.; and Xie, X. 2023. Diffusion360: Seamless 360 degree panoramic image generation based on diffusion models. *arXiv preprint arXiv:2311.13141*.
- Ghosal, D.; Majumder, N.; Mehrish, A.; and Poria, S. 2023. Text-to-audio generation using instruction-tuned llm and latent diffusion model. *arXiv preprint arXiv:2304.13731*.
- He, Y.; Yang, S.; Chen, H.; Cun, X.; Xia, M.; Zhang, Y.; Wang, X.; He, R.; Chen, Q.; and Shan, Y. 2023. Scalecrafter: Tuning-free higher-resolution visual generation with diffusion models. In *The Twelfth International Conference on Learning Representations*.
- Heusel, M.; Ramsauer, H.; Unterthiner, T.; Nessler, B.; and Hochreiter, S. 2017. Gans trained by a two time-scale update rule converge to a local nash equilibrium. *Advances in neural information processing systems*, 30.
- Ho, J.; Jain, A.; and Abbeel, P. 2020. Denoising diffusion probabilistic models. *Advances in neural information processing systems*, 33: 6840–6851.
- Ho, J.; Salimans, T.; Gritsenko, A.; Chan, W.; Norouzi, M.; and Fleet, D. J. 2022. Video diffusion models. *Advances in Neural Information Processing Systems*, 35: 8633–8646.
- Huang, R.; Huang, J.; Yang, D.; Ren, Y.; Liu, L.; Li, M.; Ye, Z.; Liu, J.; Yin, X.; and Zhao, Z. 2023. Make-an-audio: Text-to-audio generation with prompt-enhanced diffusion models. In *International Conference on Machine Learning*, 13916–13932. PMLR.
- Jiménez, Á. B. 2023. Mixture of diffusers for scene composition and high resolution image generation. *arXiv preprint arXiv:2302.02412*.
- Karras, T.; Laine, S.; and Aila, T. 2019. A style-based generator architecture for generative adversarial networks. In *Proceedings of the IEEE/CVF conference on computer vision and pattern recognition*, 4401–4410.
- Karras, T.; Laine, S.; Aittala, M.; Hellsten, J.; Lehtinen, J.; and Aila, T. 2020. Analyzing and improving the image quality of stylegan. In *Proceedings of the IEEE/CVF conference on computer vision and pattern recognition*, 8110–8119.
- Kingma, D. P.; and Welling, M. 2013. Auto-encoding variational bayes. *arXiv preprint arXiv:1312.6114*.
- Kobyzev, I.; Prince, S. J.; and Brubaker, M. A. 2020. Normalizing flows: An introduction and review of current methods. *IEEE transactions on pattern analysis and machine intelligence*, 43(11): 3964–3979.
- Lee, Y.; Kim, K.; Kim, H.; and Sung, M. 2023. Syncdiffusion: Coherent montage via synchronized joint diffusions. *Advances in Neural Information Processing Systems*, 36: 50648–50660.
- Lin, C.-H.; Gao, J.; Tang, L.; Takikawa, T.; Zeng, X.; Huang, X.; Kreis, K.; Fidler, S.; Liu, M.-Y.; and Lin, T.-Y. 2023. Magic3d: High-resolution text-to-3d content creation. In *Proceedings of the IEEE/CVF Conference on Computer Vision and Pattern Recognition*, 300–309.
- Liu, H.; Chen, Z.; Yuan, Y.; Mei, X.; Liu, X.; Mandic, D.; Wang, W.; and Plumbley, M. D. 2023. Audioldm: Text-to-audio generation with latent diffusion models. *arXiv preprint arXiv:2301.12503*.
- Liu, Y.; Zhang, K.; Li, Y.; Yan, Z.; Gao, C.; Chen, R.; Yuan, Z.; Huang, Y.; Sun, H.; Gao, J.; et al. 2024. Sora: A review on background, technology, limitations, and opportunities of large vision models. *arXiv preprint arXiv:2402.17177*.
- Nichol, A. Q.; and Dhariwal, P. 2021. Improved denoising diffusion probabilistic models. In *International conference on machine learning*, 8162–8171. PMLR.
- Podell, D.; English, Z.; Lacey, K.; Blattmann, A.; Dockhorn, T.; Müller, J.; Penna, J.; and Rombach, R. 2023. Sdxl: Improving latent diffusion models for high-resolution image synthesis. *arXiv preprint arXiv:2307.01952*.
- Poole, B.; Jain, A.; Barron, J. T.; and Mildenhall, B. 2022. Dreamfusion: Text-to-3d using 2d diffusion. *arXiv preprint arXiv:2209.14988*.
- Radford, A.; Kim, J. W.; Hallacy, C.; Ramesh, A.; Goh, G.; Agarwal, S.; Sastry, G.; Askell, A.; Mishkin, P.; Clark, J.; et al. 2021. Learning transferable visual models from natural language supervision. In *International conference on machine learning*, 8748–8763. PMLR.
- Ramesh, A.; Dhariwal, P.; Nichol, A.; Chu, C.; and Chen, M. 2022. Hierarchical text-conditional image generation with clip latents. *arXiv preprint arXiv:2204.06125*, 1(2): 3.
- Rombach, R.; Blattmann, A.; Lorenz, D.; Esser, P.; and Ommer, B. 2022. High-resolution image synthesis with latent diffusion models. In *Proceedings of the IEEE/CVF conference on computer vision and pattern recognition*, 10684–10695.
- Saharia, C.; Chan, W.; Saxena, S.; Li, L.; Whang, J.; Denton, E. L.; Ghasemipour, K.; Gontijo Lopes, R.; Karagol Ayan, B.; Salimans, T.; et al. 2022. Photorealistic text-to-image diffusion models with deep language understanding. *Advances in neural information processing systems*, 35: 36479–36494.
- Schuhmann, C.; Beaumont, R.; Vencu, R.; Gordon, C.; Wightman, R.; Cherti, M.; Coombes, T.; Katta, A.; Mullis, C.; Wortsman, M.; et al. 2022. Laion-5b: An open large-scale dataset for training next generation image-text models. *Advances in Neural Information Processing Systems*, 35: 25278–25294.
- Sohl-Dickstein, J.; Weiss, E.; Maheswaranathan, N.; and Ganguli, S. 2015. Deep unsupervised learning using nonequilibrium thermodynamics. In *International conference on machine learning*, 2256–2265. PMLR.
- Song, J.; Meng, C.; and Ermon, S. 2020. Denoising diffusion implicit models. *arXiv preprint arXiv:2010.02502*.
- Song, Y.; Sohl-Dickstein, J.; Kingma, D. P.; Kumar, A.; Ermon, S.; and Poole, B. 2020. Score-based generative modeling through stochastic differential equations. *arXiv preprint arXiv:2011.13456*.
- Tang, L.; Jia, M.; Wang, Q.; Phoo, C. P.; and Hariharan, B. 2023. Emergent correspondence from image diffusion. *Advances in Neural Information Processing Systems*, 36: 1363–1389.

Van Den Oord, A.; Vinyals, O.; et al. 2017. Neural discrete representation learning. *Advances in neural information processing systems*, 30.

Xu, J.; Wang, X.; Cheng, W.; Cao, Y.-P.; Shan, Y.; Qie, X.; and Gao, S. 2023. Dream3d: Zero-shot text-to-3d synthesis using 3d shape prior and text-to-image diffusion models. In *Proceedings of the IEEE/CVF Conference on Computer Vision and Pattern Recognition*, 20908–20918.

Yang, D.; Yu, J.; Wang, H.; Wang, W.; Weng, C.; Zou, Y.; and Yu, D. 2023. Diffsound: Discrete diffusion model for text-to-sound generation. *IEEE/ACM Transactions on Audio, Speech, and Language Processing*, 31: 1720–1733.

Zhang, Q.; Song, J.; Huang, X.; Chen, Y.; and Liu, M.-Y. 2023. Diffcollage: Parallel generation of large content with diffusion models. In *2023 IEEE/CVF Conference on Computer Vision and Pattern Recognition (CVPR)*, 10188–10198. IEEE.

Zhou, H.; Cheng, X.; Yu, W.; Tian, Y.; and Yuan, L. 2024. HoloDreamer: Holistic 3D Panoramic World Generation from Text Descriptions. *arXiv preprint arXiv:2407.15187*.

Zhou, T.; and Tang, Y. 2024. TwinDiffusion: Enhancing Coherence and Efficiency in Panoramic Image Generation with Diffusion Models. *arXiv preprint arXiv:2404.19475*.

6 Appendix

6.1 Algorithm

As described Section 3.2, we introduce the Multi-Scale Diffusion. Here we try to provide the algorithms in details.

Algorithm 1: Pseudocode of one-time denoising in Multi-Scale Diffusion.

Input: z_t^S ▷ Noisy images at timestep t
Parameter: ω ▷ Gradient descent weight
Output: z_{t-1}^S ▷ Noisy images at timestep $t - 1$

```

1: function MULTI-SCALE DIFFUSER( $z_t^s, z_{t-1}^{s-1}$ )
2:   for  $i = 1 \rightarrow N$  do
3:      $x_{t,i}^s \leftarrow F_i(z_t^s)$  ▷ Crop window from panoramic image
4:      $x_{t-1,i}^{s-1} \leftarrow F_i'(z_{t-1}^{s-1})$ 
5:      $\hat{x}_{t,i}^s = x_{t,i}^s - \omega \nabla_{x_{t,i}^s} \|ds(\Phi(x_{t,i}^s)) - x_{t-1,i}^{s-1}\|^2$  ▷ Gradient descent (Eq. 9)
6:   end for
7:   return  $\{\hat{x}_{t,i}^s\}$ 
8: end function

1: function DENOISING ONE-STEP( $z_t^S$ )
2:   for  $s = S \rightarrow 2$  do ▷ Downsample
3:      $z_{t-1}^{s-1} \leftarrow ds(z_t^s)$ 
4:   end for
5:    $z_{t-1}^1 \leftarrow \frac{\sum_i W_i \otimes F_i^{-1}(\Phi(F_i(z_t^1)))}{\sum_i W_i}$  ▷ Apply MultiDiffusion at the lowest-resolution layer (Eq. 6)
6:   for  $s = 2 \rightarrow S$  do
7:      $\{\hat{x}_{t,i}^s\} \leftarrow \text{MULTI-SCALE DIFFUSER}(z_t^s, z_{t-1}^{s-1})$ 
8:      $z_{t-1}^s \leftarrow \frac{\sum_i W_i \otimes F_i^{-1}(\Phi(\hat{x}_{t,i}^s))}{\sum_i W_i}$  ▷ Merge images
9:   end for
10:  return  $z_{t-1}^S$ 
11: end function

```

6.2 More Qualitative Results

In this section, we provide more qualitative comparison between MultiDiffusion, SyncDiffusion and our Multi-Scale Diffusion on high-resolution panoramic image generation.



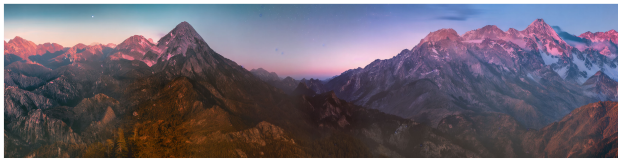
"A photo of a mountain range at twilight"



MD



Sync
Diffusion



Ours

"A photo of a lake under the northern lights"



"Clear waters and green mountains"



MD



Sync
Diffusion



Ours

"A watercolor painting of a serene seaside town"



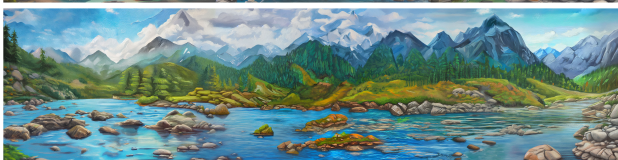
"Mountains, lakes and stones in oil paintint style illustration"



MD



Sync
Diffusion



Ours

"A photo of a lake under the northern lights"

